Classical one-dimensional Heisenberg magnet in an applied field

M. Blume*
Physics Department, Brookhaven National Laboratory, Upton, New York 11973
and State University of New York at Stony Brook, Stony Brook, New York 11794

P. Heller†
Physics Department, Brandeis University, Waltham, Massachusetts 02154

N. A. Lurie†‡
Physics Department, Brookhaven National Laboratory, Upton, New York 11973
and Physics Department, Brandeis University, Waltham, Massachusetts 02154
(Received 23 December 1974)

We present theoretical results for the thermodynamic properties and time-independent spin-spin correlation functions for the classical Heisenberg magnetic chain in an applied magnetic field. The calculations are performed by numerical solution of the transfer-matrix integral equation. In addition, approximate variational procedures and low-temperature expansions yield some analytic results. The procedures used are applicable to any near-neighbor interaction for classical spins in a linear chain. The most unusual behavior found is for antiferromagnetic coupling, where the specific heat shows oscillations as a function of field, and the longitudinal uniform susceptibility and the transverse staggered susceptibility increase with field for low fields.

I. INTRODUCTION

The physics of systems with less than three dimensions has been widely studied in recent years, especially on account of the discovery of real materials whose properties closely approximate those of one- or two-dimensional lattice models. Lower-dimensional systems have long been of theoretical interest, largely because of the relative ease in constructing models that can actually be solved—in some cases exactly. Much recent work, both experimental[1] and theoretical,[2] has focused on one-dimensional magnetic systems, with many aspects of one-dimensional magnetic behavior having already been studied. For the Heisenberg model in zero applied field, Fisher[3] provided an exact solution for the thermodynamic behavior and the static spin pair-correlation functions in the classical (infinite-spin) case. Other simple models have also been investigated, some of which have yielded exact solutions[4,5] for the static behavior.

The dynamical behavior in magnetic spin systems has long been of interest. For the case of the one-dimensional Heisenberg model in zero applied field, the dynamics has been studied theoretically,[6] largely motivated by recent neutron scattering experiments.[7,8] While much has been learned, many interesting aspects of the dynamical behavior remain unresolved. A very useful device which serves to bridge the gap between theoretical calculations and experiments on real systems is the computer "experiment."[9-12] Here one can perform an experiment on precisely the idealized model system studied theoretically. The theory can thus be tested in a way that is unencumbered by the complications of real crystals, which conform only approximately to the idealized theoretical model. Experiments of this sort on one-dimensional magnets have already provided useful information for the theorist.[11,12]

The work reported here is concerned with the thermodynamic and static correlation behavior in the one-dimensional classical Heisenberg model in the presence of an applied (uniform or "staggered") field. Our interest in this system arose in part from certain aspects of its dynamical behavior. In particular, the applied field induces a coupling between the spin fluctuations and the fluctuations in the energy density. Such a spin-energy coupling may be responsible for certain features of the neutron scattering in the ordered states of real magnetic systems undergoing phase transitions.[13] Although a phase transition does not occur in one dimension, it is of considerable interest to study the spin-energy coupling induced by the application of a field.[14,15] To study this and other aspects of the dynamical behavior in a field, a technique was developed for preparing close-to-equilibrium states of one-dimensional spin arrays. This "initialization" technique, which will be described elsewhere,[14] is a simple direct application of the present results.

Although it was motivated by our interest in dynamical studies, the present work is concerned purely with static properties. We calculated static pair-correlation functions as well as thermodynamic properties and the magnetic equation of

state. Such calculations are of experimental interest in connection with the susceptibility behavior of tetramethyl ammonium manganese chloride (TMMC) as observed in large applied fields by Walker, Dietz, Andres, and Darack.[16] Of course, as they noted, dipolar anisotropy plays a very major role in determining the magnetic behavior of TMMC, and quantum effects also enter to some extent. While we have not considered them explicitly, anisotropic terms can easily be taken into account by the techniques discussed in this paper.

We begin in Sec. II by reviewing the general features of the statistical mechanics of one-dimensional classical spin systems in the transfer-matrix formalism. This part of the discussion applies for any (translationally invariant) Hamiltonian which can be written as the sum of near-neighbor interaction terms. Here we express a number of important probability distributions and correlation functions in terms of the eigenvalues and eigenfunctions of the transfer matrix. Although a solution cannot be obtained in closed form (see Appendix B), the eigenfunctions and eigenvalues can be obtained very accurately by the numerical procedure outlined in Sec. III A. (A similar procedure was used in Ref. 16 to obtain the zero-field susceptibility in the anisotropic Heisenberg model.) We obtain the first 16 eigenfunctions and eigenvalues, and in particular we find the eigenfunction Ψ_0 belonging to the largest eigenvalue λ_0 and thus the thermodynamic properties. It turns out that, except for the case of antiferromagnetic coupling at low temperatures and moderate fields, the eigenfunction Ψ_0 is found to be remarkably well approximated by a simple exponential form. This form is then used to obtain an approximate variational solution for Ψ_0 as discussed in Sec. III B. The thermodynamic properties obtained in this variational approximation are generally very close to those of the exact (numerically obtained) eigenfunction, except as discussed in Sec. III C, where we consider explicitly the form of the eigenfunction for antiferromagnetic coupling in a field of low temperatures. Section III concludes (in part D) with an outline of the relation between the system properties in an applied "staggered" field and those in a uniform field. In Sec. IV we present selected results for the thermodynamic and static correlation properties in graphical form, and also discuss aspects of the limiting low-temperature behavior in a field.

II. TRANSFER-MATRIX FORMULATION OF THE STATISTICAL PROPERTIES OF LINEAR CHAINS

We want to solve for the thermodynamic properties and pair-correlation functions of the classical Heisenberg chain in an external magnetic field, with the Hamiltonian

$$\mathcal{H} = -J\sum_{i=1}^{N} \vec{S}_i \cdot \vec{S}_{i+1} - \frac{h}{2}\sum_i (S_i^z + S_{i+1}^z) , \tag{1}$$

where $h = \mu H$, with H the applied field and μ the magnetic moment of a spin. The spins $\vec{S}_i$ are ordinary unit vectors, and periodic boundary conditions are assumed with $\vec{S}_{N+1} = \vec{S}_1$. The transfer-matrix[5,17] method can be used to obtain both the thermodynamic properties and the correlation functions. Since the technique is applicable to more complex interactions than those in Eq. (1), we consider a more general case and only in Sec. III and in our numerical calculations do we restrict our attention to Eq. (1). We now treat the Hamiltonian with arbitrary symmetric near-neighbor interactions,

$$\mathcal{H} = -\sum_{i=1}^{N} V(\vec{S}_i, \vec{S}_{i+1}) , \tag{2}$$

where we assume

$$V(\vec{S}_i, \vec{S}_{i+1}) = V(\vec{S}_{i+1}, \vec{S}_i) .$$

Equation (1) is clearly a special case of Eq. (2) with

$$V(\vec{S}_i, \vec{S}_{i+1}) = J\vec{S}_i \cdot \vec{S}_{i+1} + \tfrac{1}{2}h(S_i^z + S_{i+1}^z) .$$

The partition function for a system governed by Eq. (2) is given by

$$Z = \int \cdots \int d\vec{S}_1 \cdots d\vec{S}_N \, e^{\beta V(\vec{S}_1, \vec{S}_2)} \times e^{\beta V(\vec{S}_2, \vec{S}_3)} \cdots e^{\beta V(\vec{S}_N, \vec{S}_1)} . \tag{3}$$

Here $d\vec{S}_i$ represents an element of solid angle of the ith spin, $d\vec{S}_i \equiv \sin\theta_i \, d\theta_i \, d\phi_i$, where θ_i and ϕ_i are the polar and azimuthal angles of that spin. Defining the kernel

$$A(\vec{S}_i, \vec{S}_{i+1}) \equiv e^{\beta V(\vec{S}_i, \vec{S}_{i+1})} ,$$

the partition function is seen to be formally the trace of the Nth power of A, which is clear if we regard the integral in (3) as the limit of a multiple summation with $\vec{S}_i$ and $\vec{S}_{i+1}$ serving as indices for the transfer of matrix A. The calculation of the trace is facilitated by the evaluation of the eigenfunctions and eigenvalues of A. Consider then the integral equation[18]

$$\int A(\vec{S}_1, \vec{S}_2) \Psi_n(\vec{S}_2) d\vec{S}_2 = \lambda_n \Psi_n(\vec{S}_1) , \tag{4}$$

which defines the eigenfunctions $\Psi_n(\vec{S})$ and eigenvalues λ_n of A. Since the eigenfunctions form a complete set [which can be assumed orthonormal, i.e., $\int \Psi_n^*(\vec{S}) \Psi_{n'}(\vec{S}) d\vec{S} = \delta_{nn'}$] the kernel A can be expanded in terms of the eigenfunctions, with the well-known result

$$A(\vec{S}_i, \vec{S}_{i+1}) = \sum_N \lambda_n \Psi_n^*(\vec{S}_i) \Psi_n(\vec{S}_{i+1}) . \tag{5}$$

Substitution of (5) into (3) and utilization of the orthonormality of the Ψ_n's then yields

$$Z=\sum_{n=0}^{\infty}\lambda_n^N \ . \tag{6}$$

In the limit of large N, only the largest eigenvalue λ_0 (which can be shown to be nondegenerate at nonzero temperatures) survives, and

$$Z\to\lambda_0^N \quad \text{for } N\to\infty \ . \tag{7}$$

A knowledge of the largest eigenvalue as a function of temperature and magnetic field can then, through Eq. (7), provide the thermodynamic functions of the system.

In order to calculate the correlation functions it is useful to define the probability distributions of the system. The probability density $W_N(\vec{S}_1,\ldots,\vec{S}_N)\times d\vec{S}_1\cdots d\vec{S}_N$, defined as the probability that the N spins of the chain point in the solid angles ranges $d\vec{S}_1,\ldots,d\vec{S}_N$ about the directions $\vec{S}_1,\cdots,\vec{S}_N$, is clearly given by

$$W_N(\vec{S}_1,\cdots,\vec{S}_N)\,d\vec{S}_1\cdots d\vec{S}_N=(1/Z)\,e^{-\beta\mathcal{H}}d\vec{S}_1\cdots d\vec{S}_N \ . \tag{8}$$

All other probability densities can be derived from this one. For example, $W_2^n(\vec{S}_1,\vec{S}_{n+1})\,d\vec{S}_1\,d\vec{S}_{n+1}$, defined as the joint probability that two spins a distance n apart along the chain point, respectively, within the ranges $d\vec{S}_1$ and $d\vec{S}_{n+1}$ about the directions $\vec{S}_1$ and $\vec{S}_{n+1}$, can be obtained from $W_N(\vec{S}_1,\cdots,\vec{S}_N)$ by integrating over all spin directions except $\vec{S}_1$ and $\vec{S}_{n+1}$. W_2^n can be expressed in terms of the eigenfunctions and eigenvalues of the transfer matrix. We have

$$\begin{aligned}W_2^n(\vec{S}_1,\vec{S}_{n+1})&=\int\cdots\int d\vec{S}_2\cdots d\vec{S}_n\,d\vec{S}_{n+2}\cdots d\vec{S}_N\,W_N(\vec{S}_1,\cdots,\vec{S}_N)\\&=\frac{1}{Z}\int\cdots\int d\vec{S}_2\cdots d\vec{S}_n\,d\vec{S}_{n+2}\cdots d\vec{S}_N\,A(\vec{S}_1,\vec{S}_2)\\&\quad\cdots A(\vec{S}_N,\vec{S}_1).\end{aligned} \tag{9}$$

Substituting Eq. (5) for A and again using the orthonormality of the eigenfunctions we find

$$W_2^n(\vec{S}_1,\vec{S}_{n+1})=\frac{1}{Z}\sum_{m,m'}\lambda_m^n\lambda_{m'}^{N-n}\Psi_{m'}(\vec{S}_1)\Psi_m^*(\vec{S}_1)\Psi_m(\vec{S}_{n+1})\Psi_{m'}^*(\vec{S}_{n+1}) \ .$$

Taking the limit $N\to\infty$, with the distance n between the spins held fixed, only the term $m'=0$ survives in the summation, and

$$W_2^n(\vec{S}_1,\vec{S}_{n+1})\to\sum_m\left(\frac{\lambda_m}{\lambda_0}\right)^n\Psi_0(\vec{S}_1)\Psi_m^*(\vec{S}_1)\Psi_m(\vec{S}_{n+1})\Psi_0^*(\vec{S}_{n+1}). \tag{10}$$

In particular, the nearest-neighbor joint probability distribution $W_2^1(\vec{S}_1,\vec{S}_2)$ is, because of Eqs. (10), (4), and (5), given by

$$W_2^1(\vec{S}_1,\vec{S}_2)=(1/\lambda_0)\Psi_0(\vec{S}_1)A(\vec{S}_1,\vec{S}_2)\Psi_0(\vec{S}_2) \ , \tag{11}$$

where the eigenfunction Ψ_0 belonging to the largest (nondegenerate) eigenvalue can be chosen to be real. Another useful probability density is $W_1(\vec{S}_1)d\vec{S}_1$, the probability that a single spin points in the range $d\vec{S}_1$ about the direction $\vec{S}_1$. This can be obtained by integrating Eq. (10) over $\vec{S}_{n+1}$:

$$\begin{aligned}W_1(\vec{S}_1)&=\int d\vec{S}_{n+1}W_2^n(\vec{S}_1,\vec{S}_{n+1})\\&=\sum_m\left(\frac{\lambda_m}{\lambda_0}\right)^n\Psi_0(\vec{S}_1)\Psi_m^*(\vec{S}_1)\int d\vec{S}_{n+1}\Psi_m(\vec{S}_{n+1})\Psi_0^*(\vec{S}_{n+1})\\&=\sum_m\left(\frac{\lambda_m}{\lambda_0}\right)^n\Psi_0(\vec{S}_1)\Psi_m^*(\vec{S}_1)\delta_{m0} \ ,\end{aligned}$$

or, finally,

$$W_1(\vec{S}_1)=\Psi_0^2(\vec{S}_1) \ . \tag{12}$$

Hence the square of the eigenfunction belonging to the largest eigenvalue has the property that it is the probability density for a single spin.

Finally, an important property of the linear chain distribution function can be obtained by defining the conditional probability $P(\vec{S}_2\,|\,\vec{S}_1)\,d\vec{S}_2$, i.e., the probability that a spin points in the solid angle range $d\vec{S}_2$ about the direction $\vec{S}_2$ *given* that its nearest neighbor points in the direction S_1. This is, by definition,

$$P(\vec{S}_2\,|\,\vec{S}_1)\,d\vec{S}_2=\frac{W_2^1(\vec{S}_1,\vec{S}_2)\,d\vec{S}_1\,d\vec{S}_2}{W_1(S_1)\,d\vec{S}_1}=\frac{A(\vec{S}_1,\vec{S}_2)\Psi_0(\vec{S}_2)\,d\vec{S}_2}{\lambda_0\Psi_0(\vec{S}_1)} \ ,$$

where we used Eqs. (11) and (12). More generally, since we employ periodic boundary conditions

$$P(\vec{S}_{i+1}\,|\,\vec{S}_i)\,d\vec{S}_{i+1}=\frac{1}{\lambda_0}A(\vec{S}_i,\vec{S}_{i+1})\frac{\Psi_0(\vec{S}_{i+1})}{\Psi_0(\vec{S}_i)}\,d\vec{S}_{i+1} \ . \tag{13}$$

This result is the basis for the "initialization" procedure used to generate equilibrium spin rings on the computer. This will be discussed in detail elsewhere.[14] For the present we point out that the Markoffian joint distribution

$$\tilde{W}(\vec{S}_1,\ldots,\vec{S}_N)\equiv W_1(\vec{S}_1)P(\vec{S}_2\,|\,\vec{S}_1)\cdots P(\vec{S}_N\,|\,\vec{S}_{N-1})$$

generated by repeated application of Eq. (13) is practically identical to $W(\vec{S}_1,\ldots,\vec{S}_N)$ for large N. Indeed, upon using (12), (13), and (5) we find

$$W(\vec{S}_1,\ldots,\vec{S}_N)=f(\vec{S}_1,\vec{S}_N)W(\vec{S}_1,\ldots,\vec{S}_N) \ , \tag{14a}$$

where

$$f(\vec{S}_1,\vec{S}_N)=\lambda_0\Psi_0(\vec{S}_1)\Psi_0(\vec{S}_N)\Big/\sum_m\lambda_m\Psi_m^*(\vec{S}_1)\Psi_m(\vec{S}_N) \ . \tag{14b}$$

In other words, the set of Markoff chains generated by repeated application of (13) corresponds exactly to the canonical ensemble for the temperature-dependent effective Hamiltonian

$$\mathcal{H}(\vec{S}_1, \ldots, \vec{S}_N) = -\sum_{i=1}^{N} V(\vec{S}_i, \vec{S}_{i+1}) - \frac{1}{\beta} \ln f(\vec{S}_1, \vec{S}_N)$$

$$= -\sum_{i=1}^{N-1} V(\vec{S}_i, \vec{S}_{i+1}) - \frac{1}{\beta}[\ln\Psi_0(\vec{S}_1) + \ln\Psi_0(\vec{S}_N)] + (\text{const}) . \tag{14c}$$

This is just the Hamiltonian for the open chain, with an effective temperature-dependent potential on the two end spins replacing the interaction between them. A detailed discussion of the effect of open-chain boundary conditions is given in Appendix A.

The correlation functions can be calculated from the probability distributions and hence are expressible in terms of the eigenfunctions and eignevalues of the transfer matrix. For example, if $f_n^{\alpha}(\vec{S})$ and $f_n^{\beta}(\vec{S})$ are arbitrary functions of the spin components at the nth site on the chain, the correlation function $\langle f_1^{\alpha}(\vec{S}_1) f_{n+1}^{\beta}(\vec{S}_{1+n})\rangle$ can be expressed

$$\langle f_1^{\alpha}(\vec{S}_1) f_{n+1}^{\beta}(\vec{S}_{1+n})\rangle = \int d\vec{S}_1\, d\vec{S}_{n+1} f_1^{\alpha}(\vec{S}_1) f_{n+1}^{\beta}(\vec{S}_{n+1}) W_2^n(\vec{S}_1, \vec{S}_{n+1})$$

$$= \sum_{m=0}^{\infty} \left(\frac{\lambda_m}{\lambda_0}\right)^n \int \Psi_n^*(\vec{S}_1) f_1^{\alpha}(\vec{S}_1) \Psi_0(\vec{S}_1)\, d\vec{S}_1 \times \int \Psi_0^*(\vec{S}_{n+1}) f_{n+1}^{\beta}(\vec{S}_{n+1}) \Psi_m(\vec{S}_{n+1})\, d\vec{S}_{n+1} . \tag{15}$$

In particular,

$$\langle S_1^z S_{n+1}^z\rangle = \sum_{m=0}^{\infty} \left(\frac{\lambda_m}{\lambda_0}\right)^n \left| \int \Psi_m^*(\vec{S}) S^z \Psi_0(\vec{S})\, d\vec{S} \right|^2 \tag{16}$$

and other correlation functions can be similarly expressed. The correlation functions are seen to fall off with distance as a sum of exponentials. Also, the average of an arbitrary function of the spin components $f(\vec{S})$ at a single site is given by

$$\langle f(\vec{S})\rangle = \int f(\vec{S}) W_1(\vec{S})\, d\vec{S} = \int f(\vec{S}) \Psi_0^2(\vec{S})\, d\vec{S}_1 , \tag{17}$$

and, in particular, the z component of the magnetization is proportional to

$$\langle S_n^z\rangle = \int S^z \Psi_0^2(\vec{S})\, d\vec{S} . \tag{18}$$

Comparison with Eq. (16) shows that the $m=0$ term in the summation in that equation is simply the square of the long-range order, i.e., $\langle S_n^z\rangle^2$.

It follows from the discussion given here that a knowledge of the largest eigenvalue and the associated eigenfunction is sufficient to provide all thermodynamic quantities and single-site spin averages. In general, the higher eigenfunctions and eigenvalues are necessary for the determination of pair-correlation functions.

III. CLASSICAL HEISENBERG CHAIN IN A FIELD

We now return to the specific problem as expressed in Eq. (1). We need the eigenvalues and eigenfunctions of the integral equation

$$\int d\vec{S}_2 \exp[\beta J \vec{S}_1 \cdot \vec{S}_2 + \tfrac{1}{2}\beta h(S_1^z + S_2^z)] \Psi_n(\vec{S}_2) = \lambda_n \Psi_n(\vec{S}_1) . \tag{19}$$

For $h=0$ the solution is straightforward; it follows from the expansion

$$e^{(\beta J \vec{S}_1 \cdot \vec{S}_2)} = 4\pi \sum_{lm} i_l(\beta J) Y_{lm}(\vec{S}_1) Y_{lm}^*(\vec{S}_2) , \tag{20}$$

where the functions $i_l(x)$ are spherical Bessel functions of imaginary argument. Comparison of Eqs. (20) and (5) shows that the eigenfunctions for $h=0$ are the spherical harmonics $Y_{lm}(\vec{S})$, and the corresponding eigenvalues are $\lambda_l = 4\pi i_l(\beta J)$, independent of m. The largest eigenvalue is obtained for $l=0$, so

$$Z \to [4\pi i_0(\beta J)]^N = 4\pi[(\sinh\beta J)/\beta J]^N .$$

This is in agreement with Fisher's solution of the linear-chain problem in zero field. The correlation functions can also be derived from the above eigenfunctions and eigenvalues, together with Eq. (15). When $h \neq 0$ the problem is no longer straightforward. The eigenfunctions for $h=0$ are independent of temperature and exchange, but this will clearly no longer be true for $h \neq 0$. The eigenfunctions do not correspond to any readily tabulated functions, and we can evaluate them either by numerical solution of the integral equation or by an analytic approximation procedure. We describe both methods in the following.

A. Numerical solution of the integral equation

Numerical evaluation of the eigenfunctions and eigenvalues is possible in practice to a very high degree of accuracy. To do this we first note that the eigenfunction can, by symmetry, be written in the form

$$\Psi_{lm}(\vec{S}) = \psi_{lm}(\cos\theta)(1/\sqrt{2\pi})\, e^{im\phi} , \tag{20a}$$

where θ and ϕ are the polar and azimuthal angles, respectively, of $\vec{S}$. We have written the index n of the eigenfunctions as the pair (l, m) to take into account the ϕ dependence of Ψ. Substituting Eq. (20a) into Eq. (19) and setting $x = \cos\theta$, the equation becomes

$$\int_{-1}^{+1} dx' \int_0^{2\pi} d\phi' \exp\left(\beta J x x' + \beta J[(1-x^2)(1-x'^2)]^{1/2}\cos(\phi-\phi') + \frac{\beta h}{2}(x+x')\right)\psi_{lm}(x')\frac{1}{\sqrt{2\pi}}e^{im\phi'} = \lambda_{lm}\psi_{lm}(x)\frac{1}{\sqrt{2\pi}}e^{im\phi} .$$

The integral over ϕ' can be carried out analytically, with the result

$$2\pi\int_{-1}^{+1} dx' \exp\left(\beta J x x' + \frac{\beta h}{2}(x+x')\right) \times I_m(\beta J[(1-x^2)(1-x'^2)]^{1/2})\psi_{lm}(x')\,dx' = \lambda_{lm}\psi_{lm}(x) . \tag{21}$$

Here,

$$I_m(x) \equiv \frac{1}{2\pi}\int_0^{2\pi} e^{x\cos\phi - im\phi}\,d\phi = I_m(-x) = I_{-m}(x)$$

is the Bessel function of imaginary argument. This one-dimensional integral equation can now be solved numerically by converting it to a matrix equation. The integral over x' is performed by N_I-point Gaussian integration, using the expression

$$\int_{-1}^{+1} f(x)dx = \sum_{j=1}^{N_I} w_j f(x_j) ,$$

where the weights w_j and points x_j are tabulated.[19] The integral equation then becomes

$$\int_{-1}^{+1} dx'\, G_m(x,x')\psi_{lm}(x') = \lambda_{lm}\psi_{lm}(x) \approx \sum_{j=1}^{N_I} w_j G_m(x,x_j)\psi_{lm}(x_j) , \tag{22}$$

where

$$G_m(x,x') = 2\pi e^{\beta J x x' + (\beta h/2)(x+x')} \times I_m(\beta J[(1-x^2)(1-x'^2)]^{1/2}).$$

If we look for solutions of Eq. (22) only at the points $x = x_i$ of the numerical integration the integral equation becomes a matrix eigenvalue equation:

$$\sum_j w_j G_m(x_i,x_j)\psi_{lm}(x_j) = \lambda_{lm}\psi_{lm}(x_i) .$$

To make this more symmetric, we multiply both sides of the equation by $\sqrt{w_i}$, obtaining

$$\sum_{j=1}^{N_I} H_{ij}^{(m)}\phi_j^{(lm)} = \lambda_{lm}\phi_i^{(lm)} , \tag{23}$$

where $H_{ij}^{(m)} = \sqrt{w_i}G_m(x_i,x_j)\sqrt{w_j}$ and $\phi_i^{(lm)} = \sqrt{w_i}\psi_{lm}(x_i)$. Equation (23) is an $N_I \times N_I$ matrix eigenvalue equation with N_I determined by the number of points used in the numerical integration. In practice $N_I = 16$ was found to give convergence to seven significant figures for all values of βJ and h for which calculations were done. The solution of Eq. (23) for given m, βJ, and h with $N_I = 16$ took about 2 sec on the Brookhaven CDC 6600 computer. Results are discussed in the following section.

The largest eigenvalue of Eq. (21) occurs for $m = 0$. (This is easily seen as a result of the fact that the eigenfunction belonging to the largest eigenvalue has no nodes.) The free energy can then be obtained from this eigenvalue, and other thermodynamic quantities can be found by numerical differentiation with respect to appropriate variables.

The z component of the magnetization $\langle S^z\rangle$ follows from Eq. (18). Since $S^z = \cos\theta = x$, we have

$$\langle S^z\rangle = \int_{-1}^{+1} dx\, x\,\psi_{00}^2(x) \approx \sum_{i=1}^{N_I} w_i x_i \psi_{00}^2(x_i) = \sum_{i=1}^{N_I} x_i(\phi_i^{00})^2 . \tag{24}$$

In the same way we can derive the following expressions for the correlation functions:

$$\langle S_i^z S_{i+n}^z\rangle = \sum_{lm}\left(\frac{\lambda_{lm}}{\lambda_{00}}\right)^n \left|\int d\vec{S}\,\Psi_{00}(\vec{S})S^z\Psi_{lm}^*(\vec{S})\right|^2 .$$

Because of the form of the eigenfunction only $m = 0$ terms survive in the summation, and

$$\langle S_i^z S_{i+n}^z\rangle = \sum_{l=0}^{\infty}\left(\frac{\lambda_{l0}}{\lambda_{00}}\right)^n \left|\int_{-1}^{+1} dx\, x\,\psi_{00}(x)\psi_{l0}(x)\right|^2 . \tag{25}$$

Note from (24) that the $l = 0$ term in this summation is simply the square of the long-range order $\langle S^z\rangle = \langle S_i^z\rangle$. Letting

$$\delta S_i^z = S_i^z - \langle S^z\rangle ,$$

we then find that

$$\langle \delta S_i^z\,\delta S_{i+n}^z\rangle = \sum_{l=1}^{\infty}\left(\frac{\lambda_{l0}}{\lambda_{00}}\right)^n \left|\int_{-1}^{+1} dx\, x\,\psi_{00}(x)\psi_{l0}(x)\right|^2 \approx \sum_{l=1}^{N_I}\left(\frac{\lambda_{l0}}{\lambda_{00}}\right)^n \left|\sum_{i=1}^{N_I} x_i\phi_i^{(00)}\phi_i^{(l0)}\right|^2 . \tag{25a}$$

Also, for the transverse correlation function,

$$\langle S_i^x S_{i+n}^x\rangle = \sum_{lm}\left(\frac{\lambda_l}{\lambda_{00}}\right)^n \left|\int dS\,\Psi_{00}(\vec{S})S^x\Psi_{lm}^*(\vec{S})\right|^2 .$$

In this case only $m = \pm 1$ survive; so

$\langle S_i^x S_{i+n}^x\rangle$

$$= \frac{1}{2}\sum_{I=1}^{\infty}\left(\frac{\lambda_{I1}}{\lambda_{00}}\right)^n \left|\int_{-1}^{+1} dx (1-x_i^2)^{1/2}\psi_{00}(x)\psi_{I1}(x)\right|^2$$

$$\approx \frac{1}{2}\sum_{I=1}^{N_I}\left(\frac{\lambda_{I1}}{\lambda_{00}}\right)^n \left|\sum_{i=1}^{N_I}(1-x_i^2)^{1/2}\phi_i^{(00)}\phi_i^{(I1)}\right|^2 . \quad (26)$$

The thermodynamic quantities of interest, such as the free energy, internal energy, isothermal susceptibility, specific heat, $(\partial M/\partial T)_h$, and adiabatic susceptibility, can also be expressed in terms of the eigenfunctions and eigenvalues of the transfer matrix. We give below the expressions which have been used in the evaluation of these quantities. The derivations follow straightforwardly from the formulas given above. (In each case we give the expression for the appropriate quantity *per spin*.)

Free energy:

$$F = -N^{-1}\beta^{-1}\ln Z = -\beta^{-1}\ln\lambda_{00} ; \quad (27)$$

internal energy:

$$E = N^{-1}\langle \mathcal{H}\rangle = -h\langle S_i^z\rangle - J\sum_i \langle \vec{S}_i\cdot\vec{S}_{i+1}\rangle , \quad (28)$$

where $\langle S_i^z\rangle$ and $\langle \vec{S}_i\cdot\vec{S}_{i+1}\rangle$ are given by Eqs. (24)–(26).

Isothermal susceptibility:

$$\chi_T = \beta N^{-1}\left\langle\left(\sum_i \delta S_i^z\right)^2\right\rangle = \beta\sum_{I=1}^{\infty}\frac{\lambda_{00}+\lambda_{I0}}{\lambda_{00}-\lambda_{I0}}C_I^2 . \quad (29)$$

Rate of change of magnetization with respect to temperature:

$$\left.\frac{\partial M}{\partial T}\right|_h = \beta^2 N^{-1}\left\langle\left(\sum_i \delta S_i^z\right)(\mathcal{H}-\langle\mathcal{H}\rangle)\right\rangle$$

$$= -\beta h\chi_T - \beta^2 J\sum_j[\langle S_i^z(\vec{S}_j\cdot\vec{S}_{j+1})\rangle - \langle S_i^z\rangle\langle\vec{S}_j\cdot\vec{S}_{j+1}\rangle]$$

$$= -\beta h\chi_T - \beta^2 J\sum_{I=1}^{\infty}\frac{2\lambda_{00}}{\lambda_{00}-\lambda_{I0}}C_I D_I . \quad (30)$$

Specific heat at constant field:

$$C_h = \beta^2 N^{-1}\langle(\mathcal{H}-\langle\mathcal{H}\rangle)^2\rangle$$

$$= \beta^2 J^2\sum_j[\langle(\vec{S}_i\cdot\vec{S}_{i+1})(\vec{S}_j\cdot\vec{S}_{j+1})\rangle$$

$$-\langle\vec{S}_i\cdot\vec{S}_{i+1}\rangle\langle\vec{S}_j\cdot\vec{S}_{j+1}\rangle] - 2h\left(\frac{\partial M}{\partial T}\right)_h - \beta h^2\chi_T$$

$$= B_0 - 2h\left(\frac{\partial M}{\partial T}\right)_h - \beta h^2\chi_T + \beta^2 J^2\sum_{I=1}^{\infty}\frac{2\lambda_{00}}{\lambda_{00}-\lambda_{I0}}D_I^2 . \quad (31)$$

Once these have been calculated, the adiabatic susceptibility can be found from the relation

$$\chi_T - \chi_S = \frac{T}{C_h}\left(\frac{\partial M}{\partial T}\right)_h^2 .$$

The coefficients B_0, C_I and D_I used above are defined by

$$C_I = \int_{-1}^{+1} dx\, x\,\psi_{00}(x)\psi_{I0}(x) , \quad (32)$$

$$D_I = \lambda_{00}^{-1}\int\int d\vec{S}\,d\vec{S}'\,\Psi_{I0}^*(\vec{S})A(\vec{S},\vec{S}')\vec{S}\cdot\vec{S}'\Psi_{00}(\vec{S}')$$

$$= 2\pi\lambda_{00}^{-1}\int_{-1}^{+1} dx\,dy\,\psi_{I0}(x)\psi_{00}(y)\exp[\beta Jxy + \tfrac{1}{2}\beta h(x+y)]\{xy - I_0(\beta J[(1-x^2)(1-y^2)]^{1/2})$$

$$+[(1-x^2)(1-y^2)]^{1/2}I_1(\beta J(1-x^2)(1-y^2)]^{1/2})\}, \quad (33)$$

$$B_0 = \langle(\vec{S}_i\cdot\vec{S}_{i+1})^2\rangle - \langle\vec{S}_i\cdot\vec{S}_{i+1}\rangle^2 = -D_1^2 + 2\pi\lambda_{00}^{-1}\int_{-1}^{+1}\int dx\,dy\,\psi_0(x)\psi_0(y)\exp[\beta Jxy + \tfrac{1}{2}\beta h(x+y)]$$

$$\times\{(1+2x^2y^2-x^2-y^2)I_0(\beta J[(1-x^2)(1-y^2)]^{1/2}) + (2xy-\beta^{-1}J^{-1})I_1(\beta J[(1-x^2)(1-y^2)]^{1/2})\} . \quad (34)$$

In addition, the following expressions for the longitudinal and transverse wave-vector-dependent susceptibilities are also easily obtained:

$$\chi^{zz}(q) = \beta\sum_{I=1}^{\infty}\frac{\lambda_{00}^2-\lambda_{I0}^2}{\lambda_{00}^2-2\lambda_{00}\lambda_{I0}\cos q+\lambda_{I0}^2}C_I^2 ,$$

$$\chi^{xx}(q) = \frac{\beta}{2}\sum_{I=1}^{\infty}\frac{\lambda_{00}^2-\lambda_{I1}^2}{\lambda_{00}^2-2\lambda_{00}\lambda_{I1}\cos q+\lambda_{I0}^2}E_I^2 ,$$

where

$$E_I = \int_{-1}^{1}\psi_{I1}(x)(1-x^2)^{1/2}\psi_{00}(x)\,dx .$$

In particular, the staggered susceptibilities may be found by setting $q=\pi$. All of these quantities are easily evaluated once the eigenfunctions and eigenvalues have been found.

B. Variational approximation for the largest eigenvalue

In some circumstances it is useful to have an analytical approximation for the eigenfunction belonging to the largest eigenvalue and an approximation for that eigenvalue which does not involve the solution to the integral equation.

For the largest eigenvalue of the integral equa-

tion (22), the variational principle gives the inequality

$$\lambda \geq \Lambda[\phi] = \frac{\int_{-1}^{+1} \int dx\, dx'\, \phi(x) G(x,x') \phi(x')}{\int_{-1}^{+1} \phi(x)^2\, dx}, \qquad (35)$$

where equality obtains when $\phi(x) = \psi_{00}(x)$. We use as a trial function $\phi(x) \propto e^{\alpha x}$ with α as a variational parameter. This form is correct for $h=0$, where $\alpha = 0$, and also for $J=0$, where $\alpha = \frac{1}{2}\beta h$. In the intermediate region, where h and J are both nonzero, this form will not be exact, but we expect it to provide a good approximation, except as explained below. We find on substituting into (35)

$$\lambda \geq \Lambda(\alpha) = \frac{2\pi\alpha}{\sinh 2\alpha} \int_{-1}^{+1} \int dx\, dy\, e^{\alpha(x+y)} e^{\beta J x y + (\beta h/2)(x+y)} \times I_0(\beta J[(1-x^2)(1-y^2)]^{1/2}). \qquad (36)$$

The integral over y can be performed, yielding

$$\lambda \geq \Lambda(\alpha) = \frac{4\pi\alpha}{\sinh 2\alpha} \int_{-1}^{+1} dx\, e^{x(\alpha+\beta h/2)} \frac{\sinh z}{z}, \qquad (37)$$

where

$$z = [(\alpha + \beta h/2)^2 + 2(\alpha + \beta h/2)\beta J x + \beta^2 J^2]^{1/2}.$$

This expression for $\Lambda(\alpha)$ is easily maximized numerically, as a function of α, and, with this value of α, the variational magnetization is calculated to be

$$\langle S^z \rangle_{\text{var}} = \coth 2\alpha - 1/2\alpha. \qquad (38)$$

In addition, it is possible to carry out the integration in (37) in a series of Bessel functions.[25] The numerical procedure was used in preference to analytical expressions, however.[26] The free energy and magnetization obtained by this procedure are accurate to better than 1% (except for the case of antiferromagnetic coupling at temperatures less than $0.2|J|$ and at fields of the order of $|J|$, as discussed in the next section).

In Figs. 1 and 2 we show the variational eigenfunction and the exact numerical solution for two values of field, temperature, and exchange. The agreement is clearly very good.

C. Asymptotic form for the eigenfunction at low temperatures

In the preceding section it was mentioned that the exponential trial form for the eigenfunction belonging to the largest eigenvalue did not work well at low temperatures for the case of antiferromagnetic coupling in a field. The physical reason for this is that the magnetization in this case is not saturated, even at very low temperatures, in fields of the order of the exchange interaction (see Sec. IV). We then expect that the probability distribution for the spins [the square of the eigenfunction according to Eq. (12)] will be strongly peaked at a value of $\cos\theta < 1$. The exponential form cannot produce such a peak, and a more detailed analysis is required.

The asymptotic form for the eigenfunction belonging to the largest eigenvalue can be found from Eq. (21) with $m=0$. Using the asymptotic form for the Bessel function $I_0(x) \sim e^{|x|}/\sqrt{2\pi|x|}$, that equation becomes

$$\left(\frac{2\pi}{\beta|J|}\right)^{1/2} \int_{-1}^{+1} dy\, \frac{\exp \beta J x y + (\beta h/2)(x+y) + \beta|J|[(1-x^2)(1-y^2)]^{1/2}}{[(1-x^2)(1-y^2)]^{1/4}} \psi(y) = \lambda \psi(x), \quad \beta \gg 1. \qquad (39)$$

The argument of the exponential peaks for $x=y=a$, where a is to be determined. Expanding that argument gives

$$\phi(x,y) \equiv \beta J x y + \frac{\beta h}{2}(x+y) + \beta|J|[(1-x^2)(1-y^2)]^{1/2} \approx \phi(a,a) + (x-a)\frac{\partial\phi}{\partial x} + (y-a)\frac{\partial\phi}{\partial y} + \tfrac{1}{2}(x-a)^2 \frac{\partial^2\phi}{\partial x^2} + \tfrac{1}{2}(y-a)^2 \frac{\partial^2\phi}{\partial y^2} + (x-a)(y-a)\frac{\partial^2\phi}{\partial x\,\partial y},$$

and, setting $\partial\phi/\partial x = \partial\phi/\partial y = 0$, we find

$$a(J - |J|) = -\tfrac{1}{2}h. \qquad (40)$$

This procedure is then valid for antiferromagnetic coupling, where $J = -|J|$, and for $h/4|J| < 1$, where we find

$$a = h/4|J| \quad \text{(antiferromagnetic coupling)}. \qquad (41)$$

For $h/4|J| > 1$, the maximum of the argument occurs outside the range of integration, and the linear exponential approximation becomes valid. From this point on we consider only the antiferromagnetic case.

On evaluating the second derivatives of $\phi(x,y)$, substituting $x=y=a$ in the denominator of (39), and extending the range of integration, we find

$$\int_{-\infty}^{+\infty} dy \exp\left(-\frac{1}{2}\frac{\beta|J|}{1-a^2}[(x-a)^2 + (y-a)^2 + 2(1-2a^2)(x-a)(y-a)]\right)\psi(y) = \lambda e^{-\beta|J|(1+2a^2)} \frac{\beta|J|(1-a^2)^{1/2}}{2\pi}\psi(x). \qquad (42)$$

$\psi(x)$ will also be strongly peaked at $x=a$; so we write

$$\psi(x) \approx c\, e^{-(1/2)[(x-a)/\sigma]^2}. \qquad (43)$$

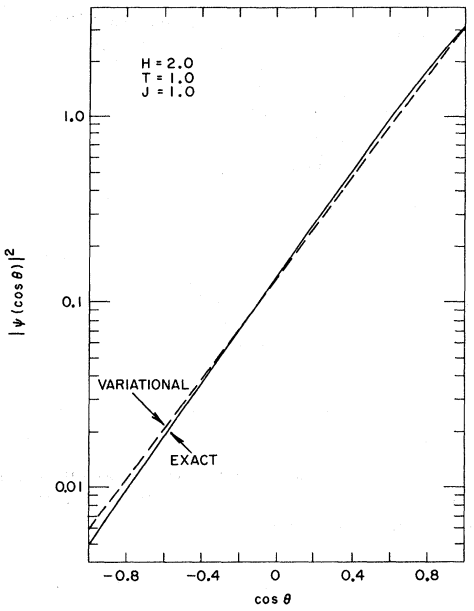

FIG. 1. Behavior of the eigenfunction belonging to the largest eigenvalue as compared with the exponential variational form for the case of ferromagnetic coupling with $k_B T/J = 1.0$ and $\mu H/J = 2.0$.

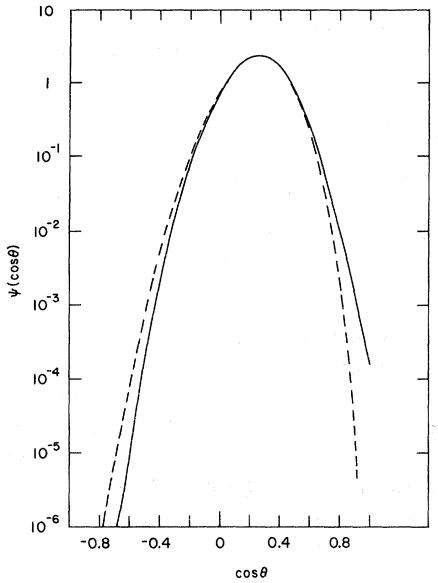

FIG. 3. Behavior of the eigenfunction belonging to the largest eigenvalue (dotted curve) as compared with the asymptotic form given in Eq. (43) (solid curve) for the case of antiferromagnetic coupling at low temperature and moderate fields. Here $k_B T/|J| = 0.03$ and $\mu H/|J| = 1$.

Substituting into (42) and carrying out the tedious algebra, we obtain expressions for σ, λ and c:

$$1/2\sigma^2 = \beta|J|a/(1-a^2)^{1/2}\,, \tag{44a}$$

$$\lambda = (2\pi/\beta|J|)\,e^{\beta|J|(1+2a^2)}[1+2a(1-a^2)^{1/2}]^{1/2}\,, \tag{44b}$$

and

$$c = (\pi\sigma^2)^{-1/2}\,,$$

where $a = h/4|J|$. In Fig. 3 we show the asymptotic low-temperature form compared with the exact solution. The agreement is quite good.

It is clear from the discussion of this section and the preceding one that the appropriate variational form for the wave function is

$$\psi(x) \propto e^{\alpha x - \gamma x^2}\,,$$

where α and γ are to be determined by maximizing (35). This procedure, with two parameters, is sufficiently cumbersome that it has no advantage over the exact solution.

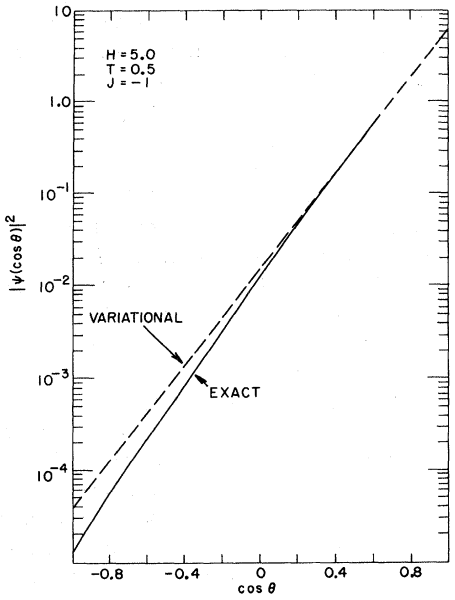

FIG. 2. Behavior of the eigenfunction belonging to the largest eigenvalue as compared with the exponential variational form for the case of antiferromagnetic coupling, with $k_B T/|J| = 0.5$, $\mu H/|J| = 5$.

D. Staggered and uniform fields

We conclude this section by noting that a simple transformation enables us to relate the solutions for ferromagnetic or antiferromagnetic coupling in a uniform magnetic field to the solutions in a staggered field. If the sign of every other spin is changed, i.e., if $\vec{S}_i \to (-)^{i+1}\vec{S}_i$, the Hamiltonian for ferromagnetic coupling in a uniform field becomes that for antiferromagnetic coupling in a staggered field, while the Hamiltonian for antiferromagnetic coupling in a uniform field becomes that for ferromagnetic coupling in a staggered

TABLE I. Equivalences between cases of staggered and uniform applied fields.

Ferromagnetic coupling, uniform field	$J \leftrightarrow -J$ $h \leftrightarrow h_{st}$ $M \leftrightarrow M_{st}$	Antiferromagnetic coupling, staggered field
Antiferromagnetic coupling, uniform field	$-J \leftrightarrow J$ $h_{st} \leftrightarrow h$ $M_{st} \leftrightarrow M$	Ferromagnetic coupling, staggered field

field. The partition function is unchanged by such a transformation, however, so the free energies in uniform and in staggered fields are equal, provided the sign of the exchange is changed. In Table I we show schematically the equivalences and changes that are possible. The calculations performed here can thus be interpreted to give a wider range of information.

IV. THERMODYNAMIC PROPERTIES AND CORRELATION FUNCTIONS. RESULTS AND DISCUSSION

Using the methods described in Sec. III, detailed results were obtained for the thermodynamic, magnetic equation of state, and longitudinal near-neighbor correlation behaviors. These are now presented in graphical form. The case of a *uniform* applied field is considered explicitly; the results for a *staggered* field may be obtained from the transformation given in Table I. Some aspects of the limiting low-temperature behavior[20] are also described.

Figure 4 shows the temperature dependence of the reduced magnetization $M/M_{sat} = \langle S^z \rangle$ for a number of different field values. The abscissa, i.e., the quantity "T" which represents the temperature,

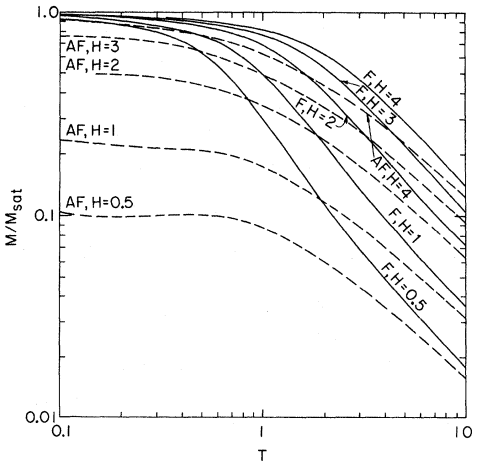

FIG. 4. Reduced magnetization as a function of $k_B T/|J|$ for different values of $\mu H/|J|$ for both ferro- and antiferromagnetic coupling.

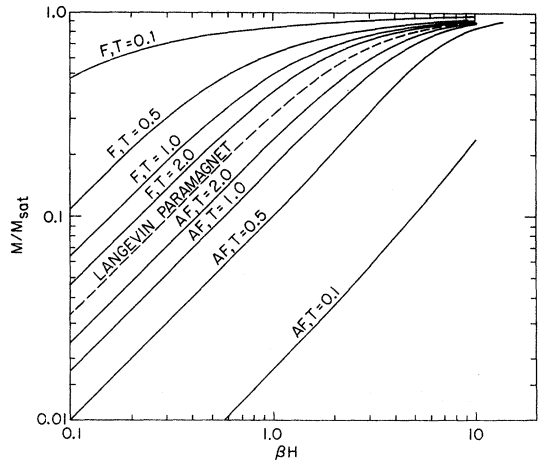

FIG. 5. Reduced magnetization as a function of $\mu H/k_B T$ for different values of $k_B T/|J|$ for both ferro- and antiferromagnetic coupling.

is the ratio[21] $k_B T/|J|$. The numbers "H" labeling the curves for different fields are values of the ratio $\mu H/|J|$. The curves labeled "F" correspond to the case of ferromagnetic coupling ($J>0$), while those labeled "AF" correspond to antiferromagnetic coupling. These notations will also be used in subsequent figures. It is seen from Fig. 4 that the magnetization generally increases as the temperature decreases at fixed field. An exception to this occurs for negative J and at low fields. Indeed, for an infinitesimal field the magnetization has a single peak at $k_B T/|J| = 0.4764$, as was already noted by Fisher.[3,21] For ferromagnetic coupling the magnetization of course saturates as $T \to 0$ °K. This is also true for antiferromagnetic coupling when $\mu H/|J| > 4$; for smaller fields, however, the limiting magnetization is given by

$$M(0\ ^\circ\mathrm{K})/M_{sat} = \mu H/4|J|\,, \tag{45}$$

as described below and in Sec. III C.

Figure 5 is a replot of the magnetization behavior. Here the abscissa is $\mu H/k_B T$, while the numbers attached to the different curves are values of $k_B T/|J|$. The dotted central curve (for which this ratio is infinity) then corresponds to the behavior of the Langevin paramagnet.

In Fig. 6 we plot the behavior of the near-neighbor correlation for the fluctuation in the longitudinal spin component, i.e., the quantity $\langle \delta S_i^z \delta S_{i+1}^z \rangle$ computed from Eq. (25a). Here the abscissa is $k_B T/|J|$, while the numbers attached to the curves are values of $\mu H/|J|$. At a given temperature the suppression of the correlation by the field is much more marked in the case of ferromagnetic coupling. (Note the factor of 2 difference in the scales for the F and AF cases.)

Figure 7 is a plot of the negative of the internal

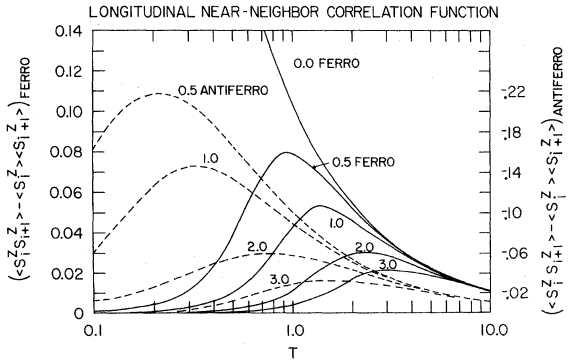

FIG. 6. Near-neighbor longitudinal correlation $\langle \delta S_i^z \delta S_{i+1}^z \rangle$ as a function of $k_B T/|J|$ for different values of $\mu H/|J|$.

energy in units of $N|J|$. The abscissa is $k_B T/|J|$, while the parameter appropriate to each curve is $\mu H/|J|$. For the case of ferromagnetic coupling (solid curves) $-E/N|J|$ tends of course to the value $1+\mu H/|J|$ in the zero-temperature limit. For antiferromagnetic coupling (dotted curves), the zero-temperature limit is given when $\mu H > 4|J|$ by

$$E(0\ ^\circ\mathrm{K})/N = |J| - \mu H, \tag{46}$$

or when $\mu H < 4|J|$ by

$$E(0\ ^\circ\mathrm{K})/N = -|J| - (\mu H)^2/8|J|\ . \tag{47}$$

These results are easily obtained by noting that for

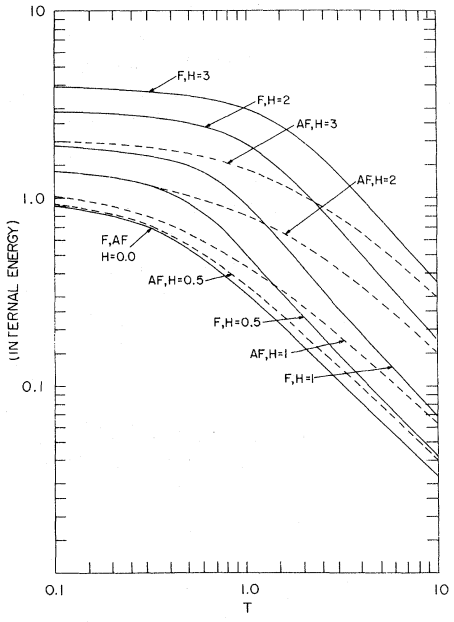

FIG. 7. Negative of the internal energy per spin in units of $|J|$ as a function of $k_B T/|J|$ for different values of $H/|J|$. Solid curves $J>0$; dotted curves $J<0$.

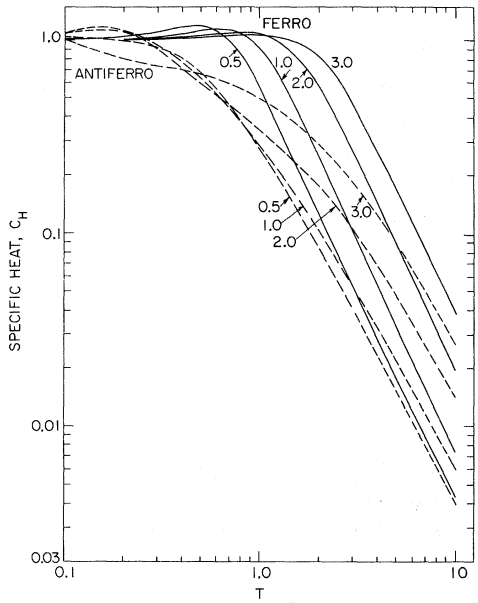

FIG. 8. Specific heat at constant field in units of Nk_B as a function of $k_B T/|J|$ for different values of $\mu H/|J|$. Solid curves $J>0$; dotted curves $J<0$.

negative J the minimum energy configurations are of the "flopped sublattice" type. Here the even- and odd-numbered spins form two sublattices, each making an angle θ with the field, the total moment being parallel to the field. The energy of such an arrangement is easily seen to be

$$E(\theta) = N|J|\cos 2\theta - N\mu H\cos\theta.$$

The angle θ_0 which minimizes this is given by

$$\cos\theta_0 = \mu H/4|J| \tag{48}$$

when $\mu H/4|J|<1$, from which Eq. (45) is easily obtained. The two sublattices become coincident when $H/4|J| \geq 1$. The expressions (47) and (46) correspond to the minimum energy value in each case. This behavior is also readily derived from the results of Sec. III C.

Figure 8 is a plot of the constant-field specific heat in units of Nk_B as a function of $k_B T/|J|$ for different values of $\mu H/|J|$. The zero-temperature limit is evidently described by

$$C_H \to Nk_B. \tag{49}$$

That this is indeed correct may be shown by separately considering the cases

(a) $J>0$,

(b) $J<0$, $\mu H > 4|J|$,

(c) $J<0$, $\mu H < 4|J|$.

In cases (a) and (b) the system ground state corresponds to full alignment of every spin with the field.

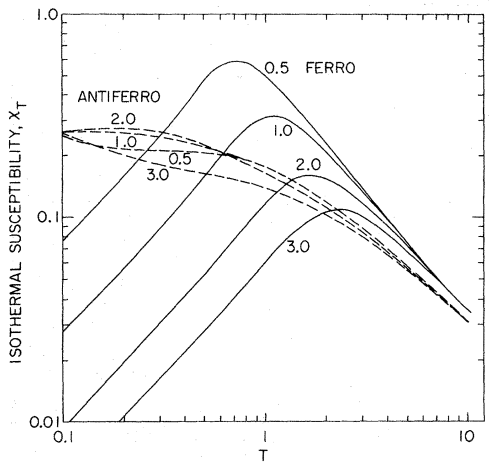

FIG. 9. Isothermal susceptibility in units of $N\mu^2/|J|$ as a function of $k_BT/|J|$ for different values of $\mu H/|J|$. Solid curves $J>0$, dotted curves $J<0$.

Then, as $T\to 0$, a spin-wave description becomes appropriate. Here we can specify the deviation of each spin from the z direction by the variable $S_n^+ = S_n^x + iS_n^y$, with

$$1 - S_n^z \cong |S_n^+|^2/2. \tag{50}$$

Then, writing

$$S_K^+ = N^{-1/2}\sum_{n=1}^{N} S_n^+ e^{iKna} \equiv U_K + iV_K, \tag{51}$$

the system Hamiltonian becomes

$$\mathcal{H}(U_1, \ldots U_N, V_1, \ldots V_N) = -NJ - N\mu H + \sum (U_K^2 + V_K^2) W(K)/2 \tag{52}$$

to terms quadratic in the spin deviations. Here

$$W(K) = \mu H + 2J(1 - \cos Ka).$$

Since the sum in (51) extends over the N wave vectors in the Brillouin zone $-\pi/a < K < \pi/a$, the result (49) follows from the equipartition theorem.

For case (c) the spin-wave analysis breaks down since there are modes for which $W(K)\to 0$ when $K\to \pi/a$. In this case, however, we can employ the results of Sec. IIIC. Using Eq. (44b), we find that in the low-temperature limit the free energy becomes asymptotically

$$F = -k_BT \ln \chi^N = -Nk_BT \ln T + C_1T + C_2,$$

where C_1 and C_2 depend only on H, J, or N. Then, writing $C_H = -T(\partial^2 F/\partial T^2)_H$, we again obtain the result (49).

Figure 9 is a plot of the isothermal susceptibility in units of $N\mu^2/|J|$ as a function of $k_BT/|J|$ for different values of $\mu H/|J|$. For the case of ferromagnetic coupling, the susceptibility at first increases strongly with decreasing temperature, very nearly as it does in zero applied field, and then drops off sharply as the system becomes saturated. The behavior in the latter region is described rather well by spin-wave theory, according to which

$$\frac{\chi_T}{N\mu^2/J} = \frac{1}{4}\frac{k_BT}{J}\left(\frac{\mu H}{J}\right)^{-3/2}\left(1+\frac{\mu H}{2J}\right)\left(1+\frac{\mu H}{4J}\right)^{-3/2}. \tag{53}$$

For $k_BT/J < 0.2$, this holds to within 7% for all points on the solid curves of Fig. 9. Equation (53) is easily obtained classically by using (50) together with the inverse of (51) to give

$$1 - \langle S^z\rangle = (2N)^{-1}\sum_K |S_K^+|^2. \tag{54}$$

Using (52), the thermal average on the right-hand side of (54) is easily performed, yielding

$$1 - \langle S^z\rangle = \frac{1}{N}\frac{k_BT}{W(K)} = \frac{k_BT}{2\pi/a}\int_{-\pi/a}^{\pi/a}\frac{dK}{\mu H + 2J(1-\cos Ka)}.$$

Carrying out the integration, we find

$$1 - \langle S^z\rangle = k_BT[(\mu H + 4J)\mu H]^{-1/2}, \tag{55}$$

which upon differentiation leads to (53). Note of course that the spin-wave approximation will break down at any given low temperature when the field becomes sufficiently small. This should happen when the susceptibility predicted by (53) is comparable to the zero-field susceptibility. Using Fisher's low-temperature limiting result $\chi_T(H=0) \propto 1/T^2$, and assuming that μH is not large compared with J, we find that this happens when

$$k_BT\left[\mu H\left(J+\frac{\mu H}{4}\right)\right]^{-1/2} \approx 1. \tag{56}$$

In the spin-wave limit the left-hand side of (56) is simply the mean-squared angular deviation of a single spin from alignment with the field. Equation (56) actually provides a rather good account of the loci of susceptibility maxima in the temperature-field plane for the case of ferromagnetic coupling.

The low-temperature-susceptibility behavior for the case of antiferromagnetic coupling is also quite interesting. From (48) we see that for $T=0$ the susceptibility has a constant value

$$\chi_T(0\,^\circ\mathrm{K}) = N\mu^2/4|J| \tag{57}$$

for $\mu H < 4J$. It should then vanish abruptly for $\mu H > 4J$, since the system becomes saturated. It is interesting to contrast this with the corresponding zero-field behavior[3]

$$\chi_T = \frac{N\mu^2}{6|J|}\left(1+\frac{k_BT}{2|J|}+\cdots\right). \tag{58}$$

Comparing (57) and (58) it is clear that if we were to plot the susceptibility as a function of the field at a fixed low temperature, a crossover must occur

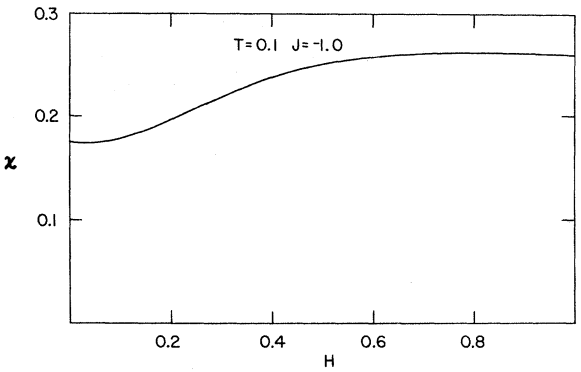

FIG. 10. Isothermal susceptibility in units of $N\mu^2/|J|$ as a function of $\mu H/|J|$ for $k_BT/|J|=0.2$ in the case of antiferromagnetic coupling. The crossover between the low-temperature behaviors described by Eqs. (58) and (57) is evident.

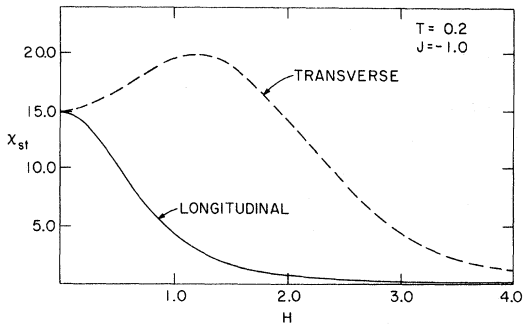

FIG. 12. Behavior of the longitudinal (solid) and transverse (dotted) staggered susceptibilities in units of $N\mu^2/|J|$ as a function of $\mu H/|J|$ for the case of antiferromagnetic coupling at $k_BT/|J|=0.2$.

between a value close to $N\mu^2/6|J|$ at $H=0$ to a roughly constant value close to $N\mu^2/4|J|$ for intermediate fields. This must in turn be followed by a rapid susceptibility decrease when $\mu H \simeq 4|J|$, corresponding to the angular coincidence of the sublattices. This may be seen in Fig. 10, where we plot the behavior of χ_T (in units of $N\mu^2/|J|$) as determined from our numerical solution carried out for $k_BT/|J|=0.1$. The crossover, though gradual, is centered at $\mu H/k_BT \approx 3$. Similar behavior was observed at $k_BT/|J|=0.2$. Note in this connection from Eq. (44a) that at low temperatures the peaked Gaussian form for the Ψ_{00} should begin to develop when $\mu H \gtrsim 3k_BT$.

The behavior of the constant-field specific heat during these processes is shown in Fig. 11 for $k_BT/|J|=0.2$. Here the abscissa is $\mu H/|J|$ and the ordinate is C_H/Nk_B. The behavior here is complicated. Finally we show in Fig. 12 the behavior of the longitudinal and transverse staggered susceptibilities as a function of applied uniform field for antiferromagnetic coupling at $k_BT/|J|=0.2$.

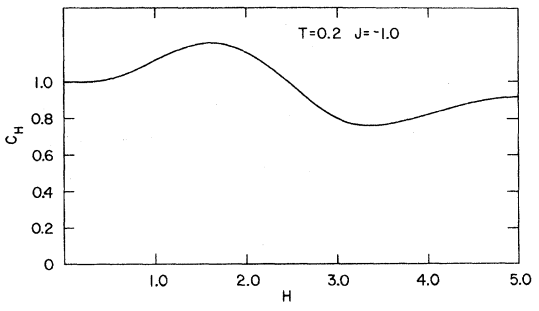

FIG. 11. Behavior of the specific heat at constant field (in units of Nk_B) as a function of $\mu H/|J|$ for the case of antiferromagnetic coupling at $k_BT/|J|=0.2$.

The most interesting feature is that the transverse staggered susceptibility *increases* with a small applied field while the longitudinal staggered susceptibility, as expected, decreases monotonically.

Some insight into the behavior of the transverse staggered susceptibility can be obtained with the results of Sec. III C. Consider the conditions under which Ψ_0 takes on the Gaussian-peaked form corresponding to the "flopped sublattice" spin configurations: At a given low temperature this generally requires that the width σ given by (44a) be small. However when $a=\mu H/4|J|$ is close to 1, the more stringent condition $\sigma \ll 1-a$ must clearly be imposed. Then (44a) yields the condition

$$k_BT/|J| \ll a \lesssim 1-3(k_BT/J)^{2/3}. \tag{59}$$

If now we define

$$\vec{T}_n=(-1)^n(\hat{x}S_n^x+\hat{y}S_n^y),$$

it is clear that when (59) holds the vectors $\vec{T}_n$ will be highly correlated ferromagnetically in going from one site to the next. Thus, letting ξ_n denote the angle between $\vec{T}_n$ and $\vec{T}_0$, the directional correlation $\langle\cos\xi_n\rangle$ must clearly become long ranged at low temperatures. Now let

$$\Delta\xi_n=\xi_n-\xi_{n-1}$$

and note from the rotational symmetry about z that the bond angle $\Delta\xi_n$ will be uncorrelated with the direction of the previous spin. [See Eq. (13).] It follows that

$$\langle\cos\xi_n\rangle=\langle\cos\xi_{n-1}\cos\Delta\xi_n-\sin\xi_{n-1}\sin\Delta\xi_n\rangle$$
$$=\langle\cos\xi_{n-1}\rangle\langle\cos\Delta\xi_n\rangle,$$

and hence that

$$\langle\cos\xi_n\rangle=u^{|n|}, \tag{60}$$

where

$$u=\langle\cos\Delta\xi\rangle$$

is the average of any bond-angle cosine. The argument leading to this exponential decay of the *directional* correlation is analogous to that used by Fisher[3] for the zero-field case. Note, however, that in the present case the *spin* correlation $\langle \vec{T}_0 \cdot \vec{T}_n \rangle$ will not have a strictly exponential decay as (26) shows. However, when (59) holds, this decay will be nearly exponential since the lengths $|T_n|$ will be nearly constant. Thus since

$$|T_n| \cong \sin\theta_0 = (1-a^2)^{1/2}, \tag{61}$$

we have

$$\langle T_0^x T_n^x \rangle = \tfrac{1}{2}\langle \vec{T}_0 \cdot \vec{T}_n \rangle \cong \tfrac{1}{2} u^{|n|}(1-a^2). \tag{62}$$

From the fluctuation theorem we then obtain

$$\frac{k_B T}{\mu^2}\chi_{st}^{xx} = \sum_{n=-\infty}^{\infty}(-)^n \langle S_0^x S_n^x \rangle = \sum_{n=-\infty}^{\infty}\langle T_0^x T_n^x \rangle$$

$$\cong \frac{1-a^2}{2}\frac{1+u}{1-u} \tag{63}$$

for the transverse staggered susceptibility per spin.

To see how this diverges as $T \to 0\,^\circ\mathrm{K}$, we use Eq. (11) for the joint distribution of a neighboring pair of spins $\vec{S}_1$ and $\vec{S}_2$. Let these be specified by the polar angles θ_1 and θ_2 and the azimuthal angles ϕ_1 and ϕ_2, and let $x_1 = \cos\theta_1$ and $x_2 = \cos\theta_2$. Writing the joint distribution in the form

$$W_2^1(\vec{S}_1, \vec{S}_2)\sin\theta_1\, d\theta_1\, d\phi_1 \sin\theta_2\, d\theta_2\, d\phi_2$$
$$= \mathcal{P}(x_1, x_2, \phi_1, \phi_2)\, dx_1\, dx_2\, d\phi_1\, d\phi_2,$$

we find from (11) and (43) that $\mathcal{P}$ is sharply peaked when $x_1 = x_2 = a$ and $\phi_1 - \phi_2 = \pi$. More specifically, writing $\Delta\xi = \phi_1 - \phi_2 - \pi$, we find

$$\mathcal{P} \propto F(x_1, x_2)\exp[-\beta|J|(1-x_1^2)^{1/2}(1-x_2^2)^{1/2}$$
$$\times(1-\cos\Delta\xi)], \tag{64}$$

where $F(x_1, x_2)$ is sharply peaked at $x_1 = x_2 = a$. The energy in the exponential in (64) is simply that associated with having the transverse projections of $\vec{S}_1$ and $\vec{S}_2$ deviate from antiparallelism by an angle $\Delta\xi$. To a good approximation we have

$$\mathcal{P} \propto F(x_1, x_2)\, e^{-\beta|J|(1-a^2)\Delta\xi^2/2},$$

and hence

$$\langle \Delta\xi^2 \rangle = [\beta|J|(1-a^2)]^{-1}.$$

We then find

$$u = \langle \cos\Delta\xi \rangle \cong 1 - \tfrac{1}{2}\langle \Delta\xi^2 \rangle = 1 - [2\beta|J|(1-a^2)]^{-1},$$

so, with $\chi_0 = \mu^2/|J|$, Eq. (63) gives

$$\chi_{st}^{xx}/\chi_0 \cong 2(k_B T/J)^{-2}(1-a^2)^2 \quad (J<0). \tag{65}$$

Comparing this with the zero-field low-temperature behavior[3]

$$\chi_{st}^{xx}(H=0)/\chi_0 \cong \tfrac{2}{3}(k_B T/J)^{-2} \quad (J<0),$$

we see that at very low temperatures the effect of a small uniform field ($k_B T/|J| \ll a \ll 1$) is a 3-fold enhancement of the staggered transverse susceptibility, followed at larger fields by a rapid decrease proportional to $(1-a^2)^2$.

CONCLUSIONS

The behavior of the isotropic Heisenberg chain in a magnetic field is clearly very complex and interesting, particularly for antiferromagnetic coupling, and we have been able to provide in this paper only a sampling of our numerical results. The techniques used here are applicable, as discussed in Sec. II, to more complex near-neighbor interactions than those for which results have been presented, including anisotropic exchange interactions, biquadratic and higher-order exchange, and higher-order single-spin terms. Calculations and analytical results can be obtained for these cases as required.

ACKNOWLEDGMENTS

We are indebted to many colleagues, including J. C. Bonner, A. K. Rajagopal, S. Krinsky, L. R. Walker, R. B. Griffiths, D. Scalapino, P. Pincus, and I. S. Jacobs for informative discussions.

APPENDIX A: PROBABILITY DISTRIBUTIONS FOR THE OPEN CHAIN

In Sec. II it was shown that the probability distribution for the closed chain (i.e. for the chain with periodic boundary conditions) is not strictly Markoffian, while the distribution for the open chain is Markoffian in the thermodynamic limit. The open chain distributions are, however, not translationally invariant, as there are surface effects (or "end" effects) on the distributions, and it was found that a distribution which was both Markoffian and translationally invariant could be obtained by placing a temperature-dependent potential, proportional to the logarithm of the eigenfunction belonging to the largest eigenvalue, on each of the end spins, as in Eq. (14c).

In this appendix we give a brief discussion of the probability distributions for the open chain, including some comments on the end effects. If the Hamiltonian is given by Eq. (2), the partition function for the open chain is

$$Z = \int \cdots \int d\vec{S}_1 \cdots d\vec{S}_N e^{\beta V(\vec{S}_1, \vec{S}_2)}$$
$$\times e^{\beta V(S_2, S_3)} \cdots e^{\beta V(\vec{S}_{N-1}\vec{S}_N)}, \tag{A1}$$

which differs from (3) only in the omission of $e^{\beta V(\vec{S}_N, \vec{S}_1)}$ from the integrand. The eigenfunctions and eigenvalues are defined as in Eqs. (4) and (5),

but the integrals over $\vec{S}_1$ and $\vec{S}_N$ are different here, since they each appear only once in the integrand. The partition function is, in the thermodynamic limit,

$$Z = \lambda_0^{N-1} \left| \int \Psi_0(\vec{S}) d\vec{S} \right|^2, \tag{A2}$$

which replaces (7). The difference between (A2) and (7) is negligible when the free energy is calculated. The probability distributions $W_2(\vec{S}_i, \vec{S}_{i+1})$ and $W_1(\vec{S}_i)$ can be calculated directly. The general expressions are ($N \gg 1$)

$$W_2(S_i, S_{i+1}) = \left[\sum_n \left(\frac{\lambda_n}{\lambda_0}\right)^{i-1} \frac{c_n}{c_0} \Psi_n(S_i)\right] \frac{A(S_i, S_{i+1})}{\lambda_0} \times \left[\sum_n \left(\frac{\lambda_n}{\lambda_0}\right)^{N-i-1} \frac{c_n}{c_0} \Psi_n(S_{i+1})\right], \tag{A3}$$

where $c_n = \int d\vec{S} \Psi_n(\vec{S})$. Also,

$$W_1(\vec{S}_i) = \int d\vec{S}_{i+1} W_2(\vec{S}_i, \vec{S}_{i+1}) = \left[\sum_n \left(\frac{\lambda_n}{\lambda_0}\right)^{i-1} \frac{c_n}{c_0} \Psi_n(S_i)\right] \times \left[\sum_n \left(\frac{\lambda_n}{\lambda_0}\right)^{N-i} \frac{c_n}{c_0} \Psi_n(S_i)\right]. \tag{A4}$$

These general expressions are functions of position in the chain, and are *not* translationally invariant. In particular, at the left end of the chain (i.e., $N \gg i \sim 1$)

$$W_1(\vec{S}_i) \approx \sum_n \left(\frac{\lambda_n}{\lambda_0}\right)^{i-i} \frac{c_n}{c_0} \Psi_n(\vec{S}_i) \Psi_0(\vec{S}_i), \tag{A5}$$

$$W_2(S_i, S_{i+1}) \approx \sum_n \left(\frac{\lambda_n}{\lambda_0}\right)^{i-1} \frac{\Psi_n(\vec{S}_i) A(\vec{S}_i, \vec{S}_{i+1}) \Psi_0(S_{i+1})}{\lambda_0} \frac{c_n}{c_0}. \tag{A6}$$

At the extreme left end ($i = 1$),

$$W_1(\vec{S}_1) = \Psi_0(\vec{S}_1)/c_0. \tag{A7}$$

In the middle of the chain, on the other hand (i.e., $N \gg i \gg 1$),

$$W_2(S_i, S_{i+1}) = \Psi_0(\vec{S}_i) A(\vec{S}_i, \vec{S}_{i+1}) \Psi_0(S_{i+1})/\lambda_0, \tag{A8}$$

and

$$W_1(S_i) = |\Psi_0(S_i)|^2, \tag{A9}$$

the same results which are found for the closed chain, as expected. It is interesting to contrast Eqs. (A7) and (A9). The probability distribution of a spin varies from being proportional to $\Psi_0(\vec{S})$ at the left end to being proportional to $|\Psi_0(\vec{S})|^2$ in the interior of the chain. This "surface effect" shows that the magnetization is smaller at the surface than in the interior. This can be made quantitative by calculating

$$\langle M_i \rangle - \overline{M} = \int d\vec{S}_i W_1(S_i) S_i^z - \int d\vec{S} |\Psi_0(S)|^2 S^z, \tag{A10}$$

the difference between the magnetization at spin i (near the left end) and the magnetization $\overline{M}$ in the interior. From (A5) this is

$$\langle M_i \rangle - \overline{M} = \sum_{n=1}^{\infty} \left(\frac{\lambda_n}{\lambda_0}\right)^{i-1} \frac{c_n}{c_0} \int d\vec{S} \Psi_n(\vec{S}) S^z \Psi_0(\vec{S}),$$

where the $n = 0$ term cancels the last term on the right in (A10) and is therefore omitted. This difference decays exponentially at relatively large distances from the end since the leading term will be $n = 1$, so $\langle M_i \rangle - \overline{M} \sim e^{i \ln(\lambda_1/\lambda_0)}$. This decay is thus similar to that of the longitudinal spin-spin correlation function. Similar expressions can be given for the finite closed chain.

APPENDIX B: BISPHERICAL AND TOROIDAL COORDINATES

It is tempting to try to find an exact solution to Eq. (19) in terms of tabulated functions. Indeed, the anisotropic Heisenberg chain was solved by Joyce[5] in terms of the Green's function for the wave equation in ellipsoidal coordinates, and he showed that the eigenfunctions and eigenvalues could be expressed in terms of spheroidal wave functions.

Equation (19) can be transformed into a form similar to the zero-field equation by writing

$$\vec{\rho}_1 = \vec{S}_1 + (h/2J)\hat{e}, \quad \vec{\rho}_2 = \vec{S}_2 + (h/2J)\hat{e}, \quad \lambda' = \bar{e}(h/2J)^2 \lambda, \quad \Phi(\vec{\rho}) \equiv \Psi(\vec{S}), \tag{B1}$$

where $\hat{e}$ is a unit vector along the z axis. Substituting into (19) then gives

$$\int d\vec{\rho}_2 e^{\beta J \vec{\rho}_1 \cdot \vec{\rho}_2} \Phi_n(\vec{\rho}_2) = \lambda_n' \Phi_n(\vec{\rho}_1). \tag{B2}$$

The only difference between this equation and that for the zero-field equation is that the integration over $\vec{\rho}_2$ is now to be carried out over a unit sphere displaced from the origin by a distance $h/2J$ along the z axis. The equation would then take its simplest form in a coordinate system for which one of the isotimic surfaces is displaced. The two such coordinate systems are bispherical or toroidal coordinates.[22] Bispherical coordinates have as isotimic surfaces spheres whose centers are always displaced from the origin a distance greater than the radius. These coordinates are therefore appropriate for $h/2J > 1$. Toroidal coordinates, on the other hand, have spheres displaced less than the radius; so they are appropriate for $h/2J < 1$. Use of these systems reduces the three-dimensional integral to one over two coordinates. Unfortunately, no further simplification is possible in these "natural" coordinates for this problem since, as pointed out by Morse and Feshbach, the wave equation is not separable in these systems, and the eigenfunctions would depend in an unseparated way on both coordinates. A different demonstration of the com-

plexity of the problem has been given by Rajagopal.[23] who found a differential equation satisfied by A. This equation too was not separable in the presence of an external field.

In any event, if numerical results were required, the numerical procedure adoped above would be more useful than the evaluation of tabulated functions. Indeed, this procedure was used by Walker[24] for the anisotropic Heisenberg chain. He solved the integral equation directly insteady of using tabulated spheroidal wave functions.

Conclusions identical to ours concerning the utility of bispherical and toroidal coordinates for the problem of the chain in a field were reached by L. R. Walker.[24] We thank him for discussions of this work.

---

*Work at Brookhaven performed under the auspices of the U. S. Atomic Energy Commission; work at Stony Brook supported by the National Science Foundation.

†Work supported by the National Science Foundation Center of Excellence Grant to Brandeis University and also by NSF Grant No. GH36612.

‡Present address: IRT Corp., Post Office Box 80817, San Diego, Calif. 92138.

[1]A review of the experimental literature is given in L. J. deJongh and A. R. Miedema, Adv. Phys. 23, 1 (1974).

[2]See, for example, E. H. Lieb and D. C. Mattis, *Mathematical Physics in One Dimension* (Academic, New York, 1966), Chap. 6.

[3]M. E. Fisher, Am. J. Phys. 32, 343 (1964).

[4]See, for example, H. E. Stanley, Phys. Rev. 179, 570 (1969).

[5]G. S. Joyce, Phys. Rev. 155, 478 (1967).

[6]F. B. McLean and M. Blume, Phys. Rev. B 7, 1149 (1973); 7, 5017(E) (1973); K. Tomita and H. Mashiyama, Prog. Theor. Phys. 48, 1133 (1972); S. W. Lovesey and R. A. Meserve, Phys. Rev. Lett. 28, 614 (1972); J. Phys. C 7, 2008 (1974); other references are contained in these papers.

[7]J. Skalyo, Jr., G. Shirane, S. A. Friedberg, and H. Kobayashi, Phys. Rev. B 2, 4632 (1970).

[8]M. T. Hutchings, G. Shirane, R. J. Birgeneau, and S. L. Holt, Phys. Rev. B 5, 1999 (1972).

[9]C. S. Windsor, Proc. Phys. Soc. (London) 91, 353 (1967); in *Proceedings of the Symposium on Neutron Inelastic Scattering* (IAEA, Vienna, 1968), Vol. II, p. 83.

[10]R. E. Watson, M. Blume, and G. H. Vineyard, Phys. Rev. 181, 811 (1969).

[11]N. A. Lurie, D. L. Huber, and M. Blume, Phys. Rev. B 9, 2171 (1974).

[12]M. Blume, R. E. Watson, and G. H. Vineyard, Bull. Am. Phys. Soc. 16, 629 (1971); Phys. Lett. A 50, 397 (1975).

[13]B. I. Halperin and P. C. Hohenberg, Phys. Rev. 188, 898 (1969); P. Heller, Intern. J. Magn. 1, 53 (1970); D. L. Huber, Int. J. Quantum Chem. 5, 667 (1971).

[14]M. Blume, P. Heller, and N. Lurie (unpublished).

[15]D. L. Huber and K. Tommet, Solid State Commun. 12, 803 (1973).

[16]L. R. Walker, R. E. Dietz, K. Andres, and S. Darak, Sol. St. Commun. 11, 593 (1972).

[17]See, e.g., C. Domb, Adv. Phys. 9, 164 (1960).

[18]We note in passing that if V is not symmetric [as a result of the presence of antisymmetric exchange of the form $\vec{D}\cdot(\vec{S}_i\times\vec{S}_{i+1})$, for example], then it is necessary to consider not only the right eigenvectors Ψ_n of (4), but also the left eigenvectors Φ_n which are solutions of $\int\Phi_n(\vec{S}_1,\vec{S}_2)\,d\vec{S}_1=\lambda_n'\Phi_n(\vec{S}_2)$. The subsequent development of the theory requires little generalization of that given here.

[19]*Handbook of Mathematical Functions*, edited by M. Abromowitz and I. A. Stegun (NBS, Washington, 1964), p. 916.

[20]The behavior at zero temperature for the classical anisotropic Heisenberg chain has been discussed by C. H. Weng [thesis, Carnegie Mellon University (1968) (unpublished)].

[21]In comparing the present results with those of Ref. 3, it should be noted that the exchange constant they employ is twice our J. Accordingly, our dimensionless temperature variable $k_BT/|J|$ is twice as large as the corresponding variable used in Ref. 3.

[22]Morse and Feshback, *Methods of Theoretical Physics* (McGraw-Hill, New York, 1953), Vol. 1, p. 665.

[23]A. K. Rajagopal, Proc. Indian Acad. Sci. A 78, 13 (1973).

[24]L. R. Walker (private communication).

[25]A. K. Rajagopal (private communication).

[26]A. K. Rajagopal and M. Blume (unpublished).